IMEKO 22nd TC3, 12th TC5 and 3rd TC22 International Conferences
3 to 5 February, 2014, Cape Town, Republic of South Africa

INVESTIGATIONS OF REFERENCE SURFACE WARP AT HIGH SHOCK CALIBRATIONS

H.Volkers [1], *T. Beckmann* [1], *R. Behrendt* [2]

[1] Physikalisch-Technische Bundesanstalt (PTB), Bundesallee 100, 38116 Braunschweig, Germany
[2] Polytec GmbH, Polytec-Platz 1-7, 76337 Waldbronn, Germany
henrik.volkers@ptb.de

Abstract: This paper describes the investigation of transducer reference surface warping during high shock calibrations using a Hopkinson bar and two laser Doppler vibrometer (LDV) and one LDV in conjunction with a laser Doppler scanning vibrometer. Dipole shocks up to 80 km/s² where applied to transfer standard back to back accelerometers with and without mass loads.

Keywords: accelerometer, shock calibration, warp, vibrometer

1. INTRODUCTION

The acceleration lab at PTB performs shock calibration of transfer standard transducers according to ISO 16063-13. The acceleration of the reference surface is simultaneous measured with two heterodyne laser vibrometer heads OFV 503 with a custom modified controller Type 2502. This modification allow us to directly sample the preconditioned 40 Mhz, phase modulated interferometer signals to apply our own demodulation, differentiation and filter algorithms.

In addition to the peak transfer ratio S_{sh}we also calculate the spectral transfer ratios $\underline{S}(f_n)$ at defined frequencies [1, 2].

Since we measure simultaneously on two positions, we usually get two slightly different signals not only caused by noise, leading to the question how the reference surface warp during high shock accelerations and how this warp is affected by a mass load. One plausible cause could be an asymmetry in the transducer housing at the connector.

Target of this investigation was a reconstruction of the surface plane warp during the shock, and its influence on the sensitivities in the frequency domain.

The majority of shock transducers for peak accelerations exceeding 30 km/s² calibrated in our lab are Endevcos type 2270 transducer. Accordingly his type was chosen for the subsequent investigation.

2. FIRST EXPERIMENTAL SETUP

Figure 1 shows the vibrometer line up. One single point vibrometer was used as a reference at one fixed position on the reference surface for all measurements. The second vibrometer was replaced by a PSV 400 scanning vibrometer.

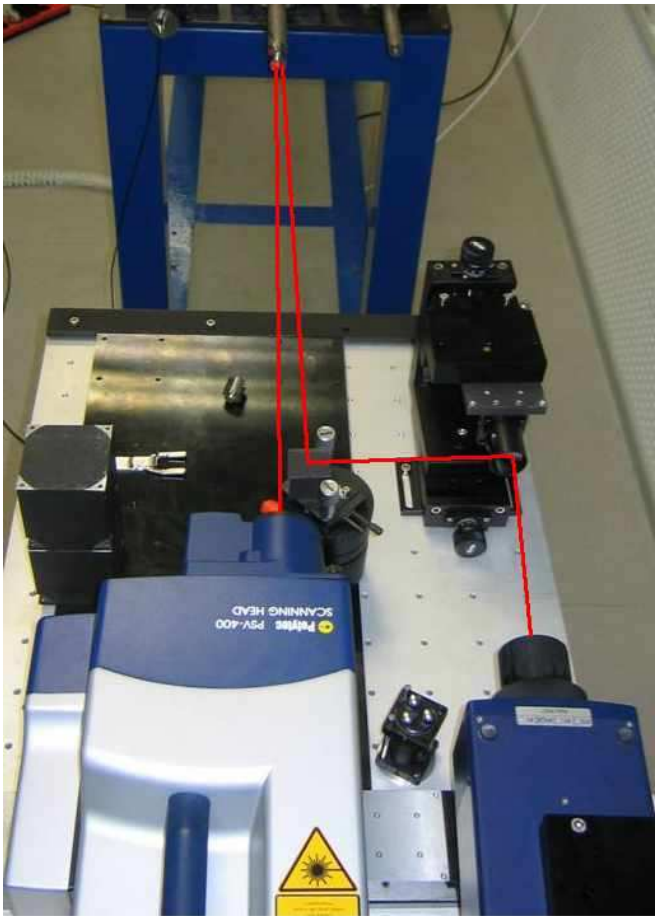

Figure 1 The scanning vibrometer and single point reference vibrometer line up. The red lines mark the laser beams targeting the transducer at the end of a 4 m Hopkinson bar.

The Sensor with a mounted mass load is shown in figure 2. To provide an insight onto the reference surface, the mass loads have four cut-outs. Picture 3 show the field of view of the scanning vibrometer with the scanning positions. The

reference position is in the cut-out at 3 o'clock, surrounded by 3 scan points.

An outer ring with 19 points was located on the Hopkinson bar, 9 points capture the reference surface in the cutouts and 8 span the mass load surface (if mounted). Figure 4 show the reconstructed planes.

The transducer was mounted with a tourque of 2.8Nm. Each measurement consists of a series of 28 or 36 shocks, the later with dummy loads.

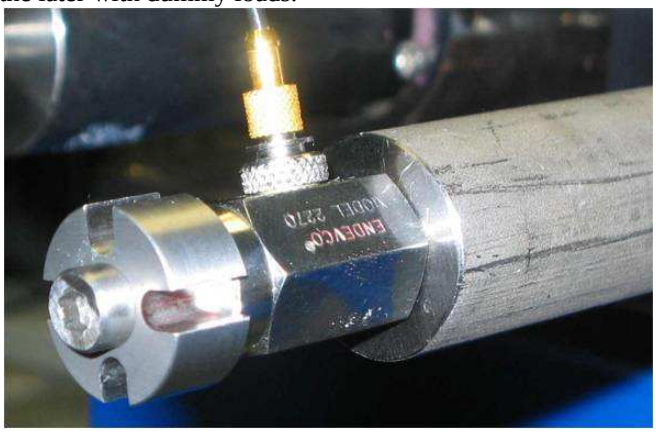

Figure 2: The tranducer mounted at the end of the Hopkinson bar with a 20 g mass load

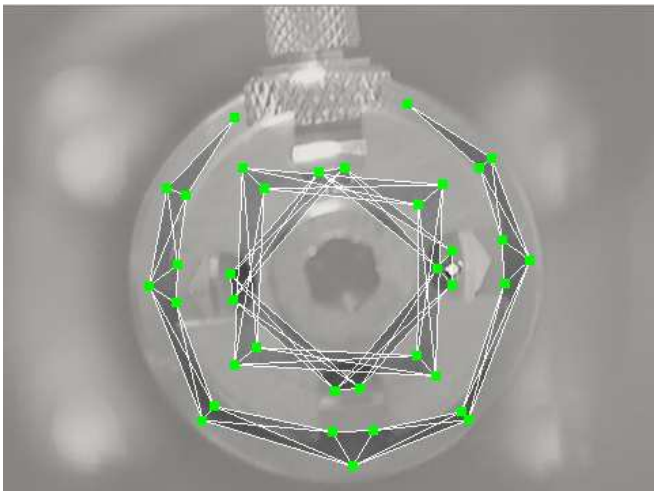

Figure 3: Field of view of the scanning vibrometer with the scan positions. The reference vibrometer laser is located in the 3 o'clock cut-out, surrounded by 3 scan positions

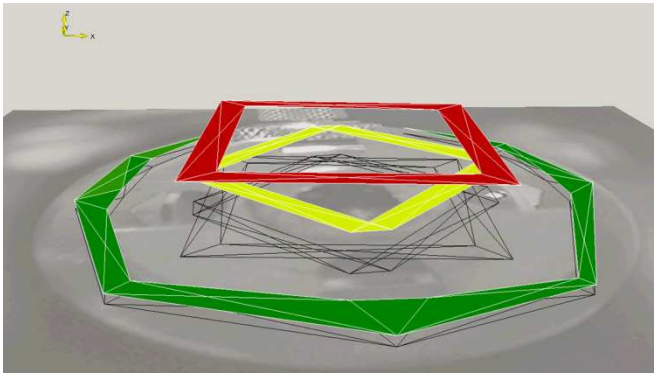

Figure 4: Reconstructed planes: Green: Bar surface: Yellow: Reference surface; Red: Top of mass load

3. DATA PREPARATION

The controller system of the scanning vibrometer was used to simultaneously capture the additional voltage signals from the analogue velocity output of the reference vibrometer and the output of the charge amplifier connected to the transducer.

Figure 5 show the acceleration profile of the reference for 28 successive shocks. The mean peak acceleration is $\bar{a}_{peak}$ = 62.9 km/s² with a relative standard deviation σ_a = 1.3%.

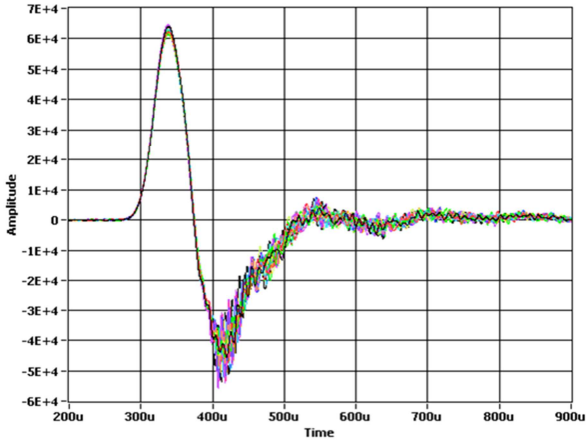

Figure 5 Reproducibility of the shock exitation. Shown is the acceleration as measured by the reference vibrometer with 28 successive shocks. Amplitude scaling in m/s², timescale in seconds

While a simple linear normalisation show acceptable results for displacement traces, the approach to align the acceleration traces by determining the transfer functions between the reference and each single scan point failed due to the low signal to noise ratio at higher frequencies and high phase variation near some modes of the housing resonances, see second setup. Figure 4 show the reconstructed planes and the attached movie (digital edition) a view of the relative motion between these planes during a shock.

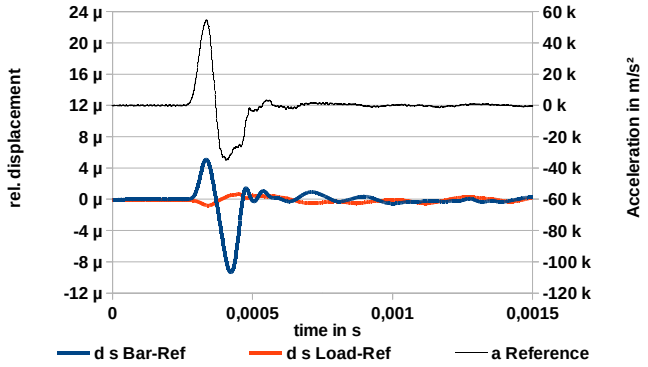

Figure 6: Movement of bar and load surface related to the reference surface. Top plot show the acceleration of the reference surface

As can be seen in Figure 6, the housing of a 2270 transducer with a 40g mass load exited with a peak acceleration of $\bar{a}_{peak}$ = 62.9 km/s² is compressed up to 5 µm and elongated up to 9 µm

4. SECOND EXPERIMANTAL SETUP

Using our regular setup with two LDVs as described in the introduction two transducers Endevco type 2270 B2B withthe SN BD47 and SN BA67 were mounted on the bar. Each transducer was exited with peak accelerations of [20, 40, 80] km/s² and measured 5 times at 4 positions A,B,C and D as shown in figure 7. In addition, these measurements were also made on the blank bar without transducer.

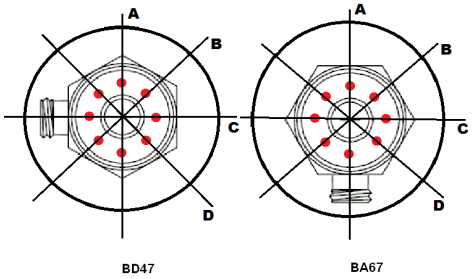

Figure 7: Laser and mounting positions of the transducer

From the two derived interferometer acceleration signals the average

$$a_{\mathrm{av}Xn}(t) = \tfrac{1}{2}\left(a_{\mathrm{IF1}Xn}(t) + a_{\mathrm{IF2}Xn}(t)\right)$$

and the differences

$$a_{\mathrm{diff}Xn}(t) = a_{\mathrm{IF1}Xn}(t) - a_{\mathrm{IF2}Xn}(t)$$

are calculated in the time domain. Index X indicate the position and n the single measurement. A DFT with a fixed rectangular window length was applied on all acceleration signals and the transducer signal $u_{Xn}(t)$. To minimize DFT leakage an algorithm looks for a minimum of the scaled, squared sum of u_{Xn}, $a_{\mathrm{IF1}Xn}$ and a_{IF2Xn} at the end of the signal, so that the start of the rectangular window is in the pre pulse region.

The complex sensitivities of the transducer

$$S_{qaXn}(\omega) = \frac{U_{Xn}(\omega)}{A_{Xn}(\omega)C(\omega)}$$

for the individual and averaged acceleration signals are calculated in the frequency domain, where $C(\omega)$ is the transfer function of the charge amplifier.

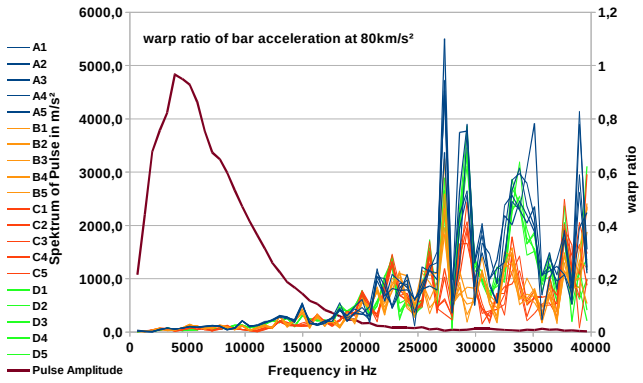

Figure 8: Amplitude spectrum of a â = 80 km/s² on a blank Hopkinson bar surface and its warp ratio.

As a measure of the surface warp, and how far it might affect the sensitivity calculation, we define the warp ratio to be the ratio of the differential and the averaged acceleration $W_{Xn}(\omega) = \frac{|A_{\mathrm{diff}Xn}|}{|A_{\mathrm{av}Xn}|}$.

Figure 8 show the amplitude spectrum of a 80 km/s² pulse on the blank bar with the resulting 20 warp ratios.

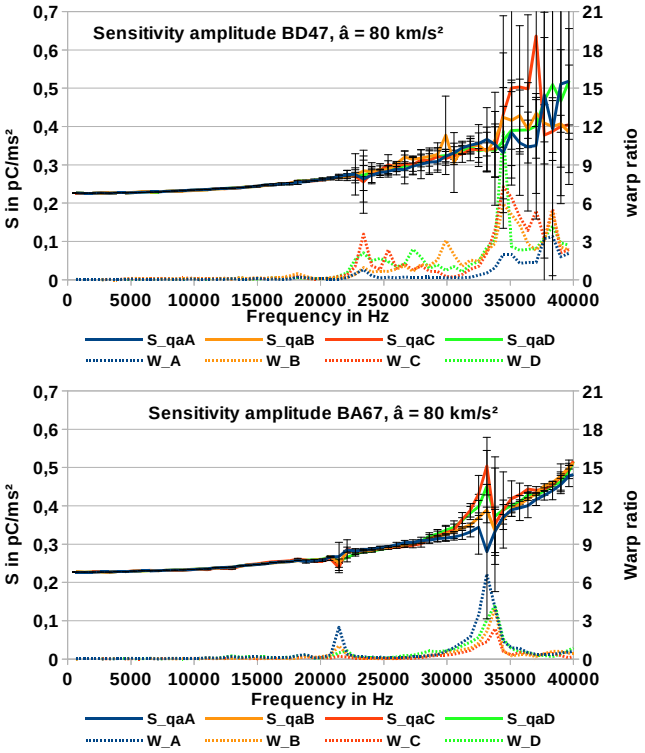

Figure 9: Sensitivity amplitude spectra of the 2270 SN BD47 (top) and SN BA67 (bottom) measured at different positions with the warp ratio on the second axis.

Figure 9 a) and b) give a more condensed view on the sensitivity amplitude spectra of both transducers investigated at $\bar{a}_{peak}$ = 80 km/s² calculated by the averaged signals at the corresponding laser positions. Each line represents the average of 5 repetitions. The uncertainty bars indicate the standard deviation expanded with k = 2,5. The warp ratios indicate position A as most sensitive to surface warp for the BA67 and position C for the BD47, which match the connector positions.

Figure 10 a) to d) show the resulting sensitivities of the individual LDV measurements in blue and green and the averaged signals in orange. The red trace correspond to the complex mean of averaged signals. The peaking of the averaged signals at the resonances might be caused by traverse sensitivity or due to slight asymmetries in the positions while aligning the laser for best SNR.

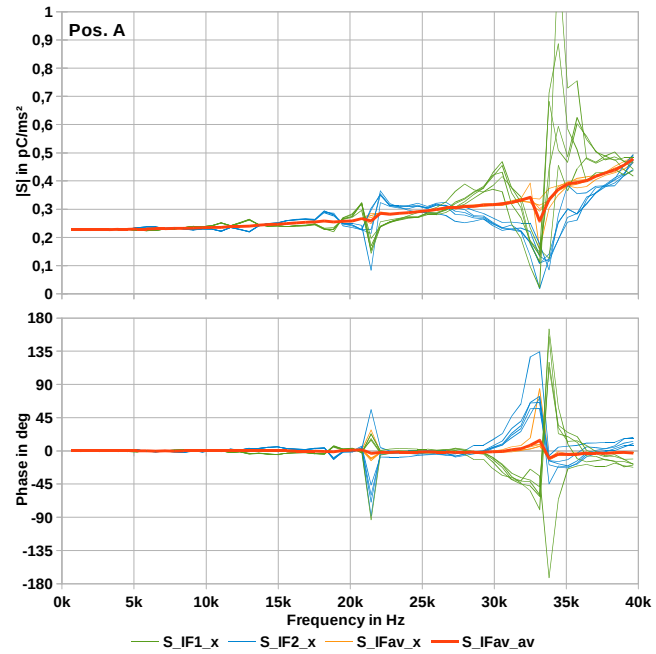

a)

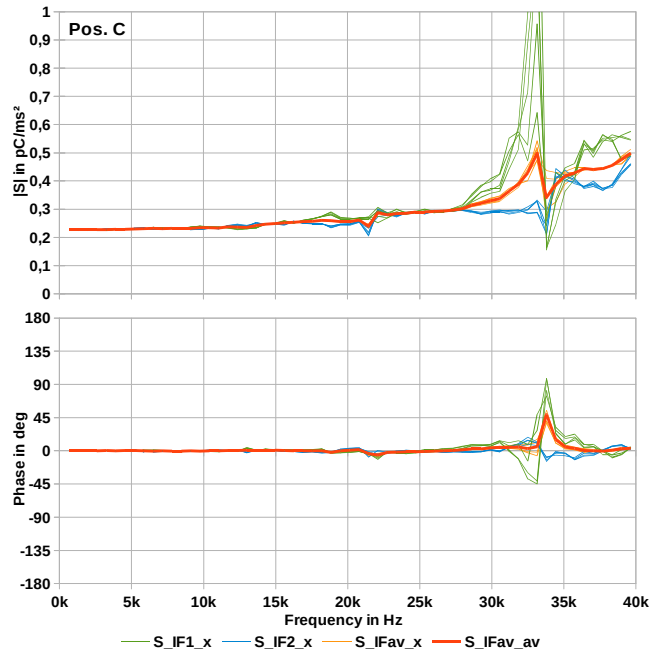

c)

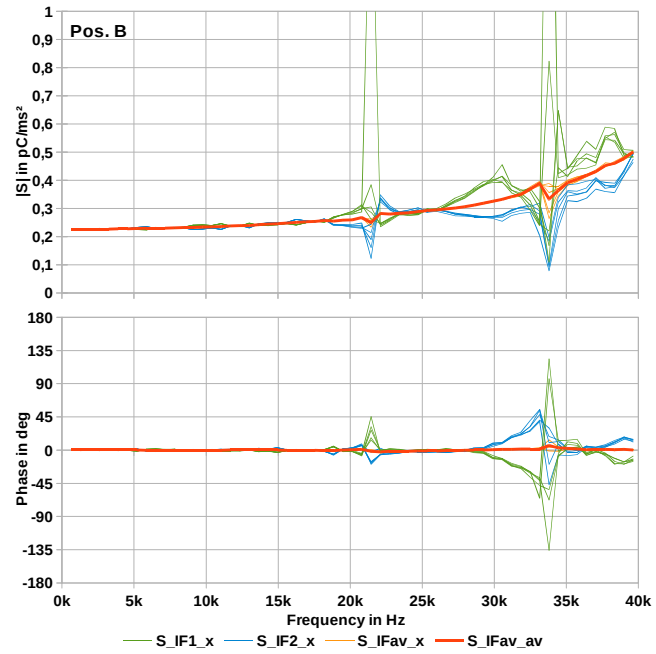

b)

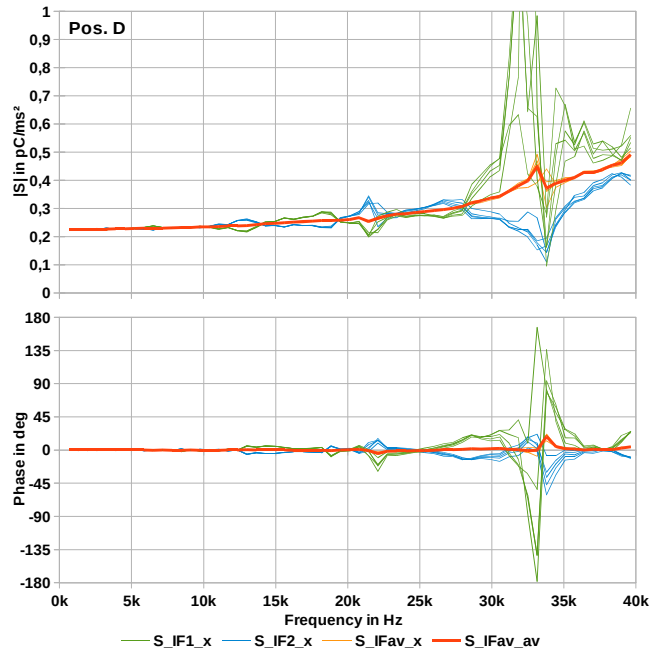

d)

Figure 10: Individual sensitivity traces of BA67 at $\bar{a}_{peak}$ = 80 km/s² a) to d) correspond to LDV positions.

5. CONCLUSION

The investigations on surface warp showed the great benefit of measuring two positions simultaneously for accelerometer (type 2270) calibration to determine the frequency response. The type and mode of the resonances found are still under investigation.

6. REFERENCES

[1] ISO 16063-13, Methods for the calibration of vibration andshock transducers,Part 13:Primary shock calibration using laserinterferometry

[2] A. Link, A. Täubner, W. Wabinsky, T. Bruns and C. Elster: “Calibration of accelerometers: Determination of amplitude and phase response upon shock excitation”, Meas.Sci.Technol. 17 (2006)